JOURNAL OF GEOPHYSICAL RESEARCH, VOL. 104, NO. D8, PAGES 9251–9260, APRIL 27, 1999

Intercomparison of cloud liquid water path derived from the GOES 9 imager and ground based microwave radiometers for continental stratocumulus

Thomas J. Greenwald

Cooperative Institute for Research in the Atmosphere, Colorado State University, Fort Collins

Sundar A. Christopher and Joyce Chou

Department of Atmospheric Sciences, University of Alabama in Huntsville

James C. Liljegren

Ames Laboratory, Ames, Iowa

Abstract. Solar reflectance measurements (0.6 and 3.9 μm) from 15-min Geostationary Operational Environmental Satellite (GOES) 9 imager data were used to estimate cloud liquid water path (LWP) for an extensive stratocumulus system over Oklahoma on May 2, 1996. The objective was to determine the consistency between these satellite estimates and retrievals from high temporal resolution (20 s) surface microwave radiometer (SMWR) measurements. The SMWRs were located at the Atmospheric Radiation Measurement (ARM) program cloud and radiation test bed (CART) sites at Morris and Purcell in Oklahoma. Results show that while the comparisons are in favorable agreement at both sites in the morning and early afternoon (root-mean-square difference of 17 g m^{-2} and correlation of 0.94), large cloud LWP maxima in the midafternoon as measured by the SMWR at the Morris site are not captured by the satellite retrievals. On the basis of indirect evidence (in situ microphysical measurements were unavailable), it is hypothesized that the discrepancies may be the result of the formation of light drizzle in the middle to lower portions of the cloud, unseen at visible and near-infrared wavelengths from space but easily sensed by microwave radiometry. These results demonstrate that extra care must be taken in future efforts to validate satellite derived cloud properties on a routine basis using SMWR data. Additional information about the cloud microphysical properties may also be required to help properly interpret the comparisons, particularly in the later stages of development of stratocumulus.

1. Introduction

Because of its strong interactions with visible and infrared radiation, cloud liquid water has been proposed to play a potentially significant role in global climate through the so-called cloud liquid water feedback [*Paltridge*, 1980; *Somerville and Remer*, 1984] and through direct solar radiative forcing [*Ramaswamy and Chen*, 1993]. Little is known about the extent to which this feedback might influence the global climate since modeling studies have yet to come to a consensus on its net effect [*Roeckner et al.*, 1987; *Taylor and Ghan*, 1992]. Crucial to understanding and predicting these effects is the validity of the global distributions of cloud liquid water produced by the new generation of climate models. Some attempts have been made to compare these model simulations with passive microwave satellite observations [e.g., *Fowler et al.* 1996; *Lemus et al.* 1997]. However, such comparisons have been limited exclusively to ocean regions where passive microwave techniques excel. There is also a need to verify the model-generated liquid water distributions over land regions as well. While it is crucial to validate climate model simulations using satellite remote sensing observations, it is equally important to validate and provide error estimates of the satellite data products themselves. This can be achieved using potentially more accurate measurements from in situ and ground-based systems while taking into account the errors associated with these systems.

While there is a long and rich heritage of estimating cloud liquid water path (LWP) over the oceans from spaceborne passive microwave sensors [e.g., *Basharinov et al.*, 1969; *Prabakhara et al.*, 1983; *Greenwald et al.*, 1993], another attractive approach for estimating cloud LWP over both land and ocean uses visible (0.6-0.75 μm) and near-infrared (1.65, 2.16, 3.7-3.9 μm) measurements to obtain the optical depth and particle size of water clouds, which we refer here as the solar reflectance (SR) method. This method exploits the different scattering behavior of solar radiation by water drops at these selected wavelengths. Applications of this method have been carried out using the advanced very high resolution radiometer (AVHRR) during the Atlantic Stratocumulus Transition Experiment (ASTEX) [*Nakajima and Nakajima*, 1995], the Multispectral Cloud Radiometer (MCR) [*Nakajima et al.*, 1991], and the Geostationary Operational Environmental Satellite (GOES) 8 imager [*Greenwald et al.*, 1997]. Using this

Paper number 1999JD900037.
0148-0227/99/1999JD900037$09.00

technique, a near-global survey of low-level water clouds has also been completed [*Han et al.*, 1994].

The SR method's major advantage is that retrievals of cloud LWP are possible with consistent accuracy over ocean and most land surfaces. The obvious main disadvantage is that retrievals are only possible during daylight hours. Other disadvantages include the retrieved drop sizes being somewhat difficult to interpret and only representative of sizes near cloud top [*Nakajima et al.*, 1991], the effects of sub-field-of-view cloud inhomogeneities [e.g., *Loeb and Coakley* 1998], and the frequent necessity for postlaunch calibration of the measurements [*Che and Price*, 1992; *Kaufman and Holben*, 1993; *Greenwald et al.*, 1997].

Perhaps not the most accurate but certainly the most precise way to remotely sense cloud LWP derives from ground-based upward looking microwave radiometers [e.g., *Westwater*, 1978]. The most commonly used radiometers consist of dual channels near the 22 GHz H_2O absorption line and the adjacent window at about 31 GHz. Limited comparisons of cloud LWP retrievals from microwave radiometers have compared well with simultaneous in situ measurements [*Hill*, 1994], though retrievals can sometimes exhibit systematic errors. These errors can usually be overcome through careful calibration procedures. Despite these problems, ground-based passive microwave systems have the distinct advantage of producing high temporal resolution measurements with near-continuous operation and are potentially an important source of validation for satellite remote sensing methods.

The focus of this study is to compare simultaneous retrievals of cloud LWP from the GOES 9 imager and upward looking microwave radiometers over land to improve the understanding of the observations obtained from these vastly different measurement systems. Other related work includes *Minnis et al.* [1992], who used GOES 7 measurements and ground-based microwave radiometer estimates of cloud LWP during the First ISCCP Regional Experiment (FIRE) to infer the effective radius of marine stratocumulus and *Han et al.* [1995], who compared spatially sampled AVHRR retrievals of cloud LWP to a limited number of ground microwave radiometer observations over San Nicolas Island during FIRE. Our study differs from this previous work mainly in that high-resolution time series are obtained from both measurement systems and that the comparisons are made over land. A comparison case consisting of a reasonably homogenous, stratocumulus system was selected over the Atmospheric Radiation Measurement (ARM) program cloud and radiation testbed (CART) sites in Oklahoma.

2. Data

The U.S. Department of Energy, through the ARM program, created a wide network of surface-based instruments over several regions of the Earth to improve the measurement of radiation in the Earth-atmosphere system [*Stokes and Schwartz*, 1994]. One of these designated regions is the United States southern Great Plains. The central facility and all boundary sites in this area each have microwave radiometers. These microwave systems have two channels (23.8 and 31.4 GHz) to simultaneously observe column water vapor and cloud LWP. The 23.8 GHz channel primarily senses water vapor, while the 31.4 GHz channel detects liquid water. Data at 20-s resolution were used from the sites at Purcell (34.97°N, 97.42°W) and Morris (35.68°N, 95.86°W) in Oklahoma (see Figure 1).

The operational water vapor and cloud LWP products are derived from a statistical retrieval technique that uses constant coefficients unique to each location's climatology [*Liljegren*, 1998]. To improve upon these retrievals, we used a modified approach that allows for these coefficients to vary according

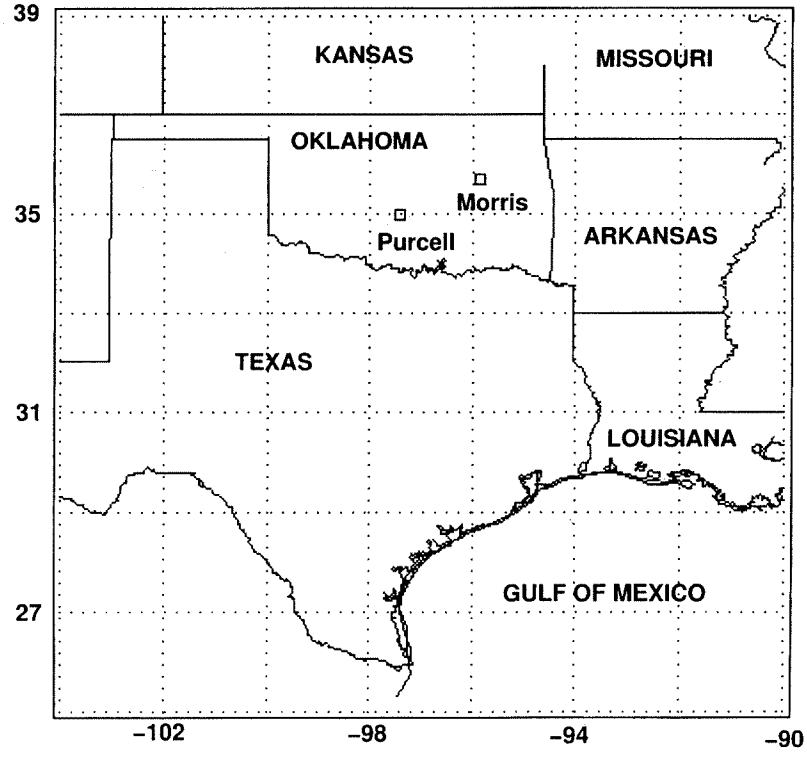

Figure 1. Area of study indicating location of surface microwave radiometers.

to changes in the oxygen and water vapor absorption and permits changes in the mean radiating temperature of the atmosphere. Given two frequencies, the column water vapor (V) and cloud LWP (L) can be expressed as a linear combination of the optical depth of water vapor plus liquid water at each frequency [*Liljegren*, 1998]:

$$V = v_1\tau'_{23} + v_2\tau'_{31}$$

$$L = l_1\tau'_{23} + l_2\tau'_{31}$$

where the coefficients v_1, v_2, l_1, and l_2 are functions of the water vapor and liquid water absorption. The coefficients v_1 and v_2 are parameterized in terms of atmospheric pressure, relative humidity, and temperature at the surface. The coefficients l_1 and l_2 are also parameterized using atmospheric pressure and relative humidity at the surface but include cloud base temperature (T_{base}) as well. Since information about T_{base} was not known, a climatic value was used. The optical depths of water vapor plus liquid water at 23.8 and 31.4 GHz (τ'_{23} and τ'_{31}, respectively) are defined at each frequency as the total optical depth (τ_t) minus the oxygen optical depth (τ_{ox}), where τ_{ox} is frequency dependent and parameterized as a function of surface temperature and atmospheric pressure. The total optical depth at frequency, ν, is expressed as

$$\tau_t(\nu) = \ln\left(\frac{T_{mr}(\nu) - T_c}{T_{mr}(\nu) - T_b(\nu)}\right)$$

where T_{mr} is the mean radiating temperature (parameterized in terms of the three surface parameters mentioned previously), T_c is the cosmic background radiating temperature (2.73 K), and $T_b(\nu)$ is the measured brightness temperature.

Although the measured brightness temperatures were carefully calibrated, the cloud LWP retrievals under clear skies were found to contain systematic errors of approximately +10 g m^{-2} at Purcell and +50 g m^{-2} at Morris. The cause of these errors is uncertain. They may be the result of biases in either τ_{ox} or T_{mr} (at 31.4 GHz) in the retrievals or possibly unknown problems in the calibration of the brightness temperatures. The data were adjusted accordingly to account for these errors.

The imagers on the GOES I series of satellites provide improved sensitivity, greater navigational accuracy, and a new higher resolution near-infrared channel that is useful for retrieving cloud particle size [*Menzel and Purdom,* 1994]. The channels and their approximate half-power bandwidths for these instruments are as follows: 1 (0.52-0.74 μm), 2 (3.79-4.04 μm), 3 (6.47-7.06 μm), 4 (10.2-11.2 μm), and 5 (11.6-12.5 μm). The effective spatial resolutions of the imager are 0.57 x 1 km for channel 1 and 2.3 x 4.0 km for channels 2, 4, and 5. This study uses data from the GOES 9 imager that is positioned on the equator at 135°W. There is some evidence to suggest that channel 1 on the GOES 8 suffers from calibration problems [*Greenwald et al.*, 1997]. As yet, a similar problem for the GOES 9 imager has not been documented; thus we rely on the prelaunch calibration data. Additional details concerning the specifications of the imager are given by *Menzel and Purdom* [1994].

The solar reflectance technique for retrieving cloud LWP uses dual solar radiation measurements at a nonabsorbing visible wavelength (0.6 μm) and a liquid water absorbing near-infrared wavelength (3.9 μm) to derive the cloud optical depth and effective droplet radius. The effective radius (r_e) is defined as

$$r_e = \frac{\int_0^\infty n(r)r^3 dr}{\int_0^\infty n(r)r^2 dr}$$

where $n(r)$ is the size distribution for drops of radius r. The 0.6-μm reflectance responds primarily to the optical depth (τ) of the cloud, whereas the 3.9-μm reflectance is sensitive to changes in r_e. A detailed theoretical discussion of this method is given by *Nakajima and King* [1990]. Limitations in the method occur for optically thin clouds composed of small droplets whereby two solutions for τ and r_e can be obtained, a consequence of water droplets losing their scattering efficiency faster for longer wavelengths as particle size decreases [*Nakajima and King*, 1990].

To apply this method, a series of bispectral grids of the reflectances at 0.6 and 3.9 μm (accounting for the spectral response of the instrument) for selected values of τ and r_e are computed for various viewing and solar geometries using a multistream discrete ordinate radiative transfer model (see *Nakajima and King* [1990] for an example of such a grid). Underlying assumptions are that the cloud droplets follow a modified gamma size distribution and that the cloud has a plane-parallel geometry. Optical properties of the water drops were computed using Lorenz-Mie theory and the spectral response curves for the GOES 9 imager. Surface reflectances of 6% and 2.5% were assumed at 0.6 μm and 3.9 μm, respectively (typical of the ocean), since the bispectral grids were already available. Land surfaces typically have larger reflectances (about 18% at 0.6 μm for the ARM sites). However, surface reflectance will only impact the retrieval of cloud properties for very optically thin clouds [*Platnick and Valero*, 1995].

Adjustments are made to the 3.9-μm measurements by accounting for the atmospheric thermal emission component and the transmission of the solar radiation by water vapor. The GOES 9 11-μm measurements (channel 4), applying the method of *Allen et al.* [1990], were used to account for the atmospheric emission. A correction factor for the transmission by water vapor was estimated using LOWTRAN 7 [*Kneizys* 1988], a low spectral resolution model for computing atmospheric transmittance. Given a viewing and solar geometry and measurements at 0.6 μm and adjusted measurements at 3.9 μm, the τ and r_e can be retrieved simultaneously by interpolating the bispectral grid. Once τ and r_e are determined, the cloud LWP follows from [e.g., *Han et al.*, 1995]

$$\text{LWP} = \frac{4\tau r_e \rho_w}{3Q_{ext}}$$

where ρ_w is the density of liquid water ($\approx 10^6$ g m^{-3}) and Q_{ext} is the average extinction efficiency over the droplet size distribution (approximately 2 at visible wavelengths).

Platnick and Valero [1995] found that for optical depth retrievals the errors are dominated by uncertainties in the visible reflectance for large τ and by uncertainties in the surface albedo for small values ($\tau < 3$). For an optical depth of 10, the typical retrieval error is roughly 18% assuming a ± 10% uncertainty in the visible measurements. Effective radius retrievals are affected principally by uncertainties in the measurements and effective variance of the cloud drop size

distribution. Total errors are expected to be about ± 25%. For a cloud with τ =10 and r_e=10 μm (LWP = 67 g m^{-2}), this translates to an error in cloud LWP of 20 g m^{-2}.

Retrievals were performed only for cloudy pixels, which were determined using multispectral GOES 9 measurements (channels 1, 2, 4, and 5) and the cloud detection scheme developed for the Clouds and Earth Radiant Energy System (CERES) project [*Baum et al.*, 1996]. The zenith angles for the Purcell and Morris sites from the GOES 9 platform are 50° and 52°, respectively. To minimize the effects of navigational errors, a 3 x 3 array of GOES 9 pixels surrounding these sites was considered in the analyses.

3. Results

On May 2, 1996, an extensive and persistent stratocumulus cloud deck developed over the eastern half of Oklahoma and Texas. Although ground observations of cloud type were not available for this study, inspection of GOES 9 visible imagery revealed that this system exhibited features characteristic of stratocumulus, such as the appearance of small cells and cumulus-type elements. These cloud conditions provided an ideal situation for comparing the satellite and SMWR observations of cloud LWP. The weak trailing surface low from previous days had pushed into Central Texas, developing a leading warm front, bringing warm humid Gulf air northward into this region. The 500-mb flow was zonal, and the combination of warm moist air at low levels, warm surface temperatures, and a lack of a strong synoptic forcing were conducive to stratiform cloud formation.

An important consideration in these comparisons is to ensure that during the study period moderate-to-heavy precipitation did not occur over the two ground sites. This is because the surface microwave radiometer (SMWR) measurements are sensitive to raindrops that can greatly bias the cloud LWP observations [*Sheppard*, 1996]. Weather radar summaries and nearby rain gauge observations indicated that measurable precipitation did not occur in the vicinity of the two sites. In addition there was no indication at either site that water had accumulated on the Teflon window protecting the radiometers. While we can eliminate the possibility of measurable precipitation occurring at these sites, we cannot discount that light rainfall, such as drizzle, may have been present aloft.

The GOES 9 observations at 15-min intervals provided a unique and detailed depiction of the time and space evolution of the LWP of this cloud system (Plate 1). Over its lifecycle, it remained remarkably stationary. Its greatest spatial extent occurred early in its history from 1600 to about 1900 UTC. Over the entire case study period, the broad region of maximum LWP values was located just south of the Morris site. The peak LWP reached about 290 g m^{-2} at 1900 UTC. Soon thereafter, a noticeable decay of the cloud system began both in terms of its areal coverage and magnitude of LWP.

Certain cloud characteristics and atmospheric conditions during this period were derived from 3-hourly radiosonde data at both sites. A summary is given in Tables 1 and 2. The cloud top height (above sea level) was defined as being near the base of the inversion in the temperature sounding, while the cloud base height was defined as the shift from a dry to moist adiabatic lapse rate in the temperature sounding. Missing data in Table 2 is due to the inability to reliably determine the height of the cloud top and/or base from the sounding. Because stratocumulus often exhibit adiabatic-like behavior since entrainment is usually not significant and is limited to cloud top [e.g., *Martin et al.*, 1994] estimates of the cloud LWP were also computed for comparison assuming adiabatic ascent of air parcels based on the method of *Albrecht et al.* [1990].

Cloud depth and adiabatic cloud LWP were generally greater at the Morris site, which is consistent with the GOES 9 images of cloud LWP (see Plate 1) that showed Morris was nearest the thickest portions of the cloud system and Purcell was at or near the cloud system boundary throughout the study period. The cloud base height was typically higher at the Purcell site because its altitude is about 127 m higher than at Morris. The inversion at Morris never became as strong as at Purcell (we define the inversion "strength" as the difference in temperature between the top and bottom of the inversion) but was maintained over a longer period of time. According to the GOES 9 imagery, conditions became clear after 1915 UTC (Plate 1) at Purcell. While the radiosonde data indicated the inversion had broken at Purcell at 2330 UTC, it is likely this event may have occurred an hour or two earlier.

To examine the time variation of the satellite-derived cloud properties, a time series of the GOES 9 retrieved optical depth and r_e are given in Figures 2a and 3a for the Morris and Purcell sites, respectively. Standard deviations of the data within the 3 x 3 grids are also shown. The most striking feature is the strong diurnal signature of cloud optical depth at the Morris site, ranging from a minimum of 3-4 at 0900 and 1530 local time to a maximum of about 20 at 1130-1230 local time. The effective radius, in contrast, remained constant (10±1 μm) throughout most of the time period. However, it experienced an increasing trend after 2100 UTC, reaching a maximum of about 16 μm. This behavior is unlike marine stratocumulus that have been shown to exhibit a moderately strong diurnal signature in effective radius [e.g., *Minnis et al.*, 1992]. Equivalent blackbody (EBB) temperatures at 11 μm also remained roughly uniform (282-285 K) with no discernable relationship with variations in the optical depth of the cloud.

At Purcell (Figure 3a) the cloud optical depth generally decreased with time in the morning except for a relative maximum near local noon, after which the conditions become clear. The 11-μm EBB temperatures (not shown) increased sharply (> 286 K) later in the morning. This was mainly due to the clouds becoming more broken in nature that allowed the penetration of surface longwave radiation. The effective radius exhibited a minor diurnal variation that closely follows that of the optical depth and the mean value was slightly smaller than at the Morris site, with values ranging from about 8 to 10 μm.

A comparison of the time series of the cloud LWP derived from the two different observation systems revealed some intriguing results (Figures 2b and 3b). The conditions at Morris were overcast from about 1615 to 2200 UTC, while Purcell was overcast during 1500-1845 UTC. At Morris, clear skies were only observed at the surface at about 1545-1600 UTC and beyond 2240 UTC (see Figure 2b). Because ceilometer observations were unavailable, clear conditions were determined using 10-min moving standard deviations of the SMWR 31.4 GHz brightness temperatures (local standard deviations less than about 0.2 K are a good indicator of water cloud free skies). Remarkably, the satellite observations capture the gross trends in the cloud LWP during the morning and

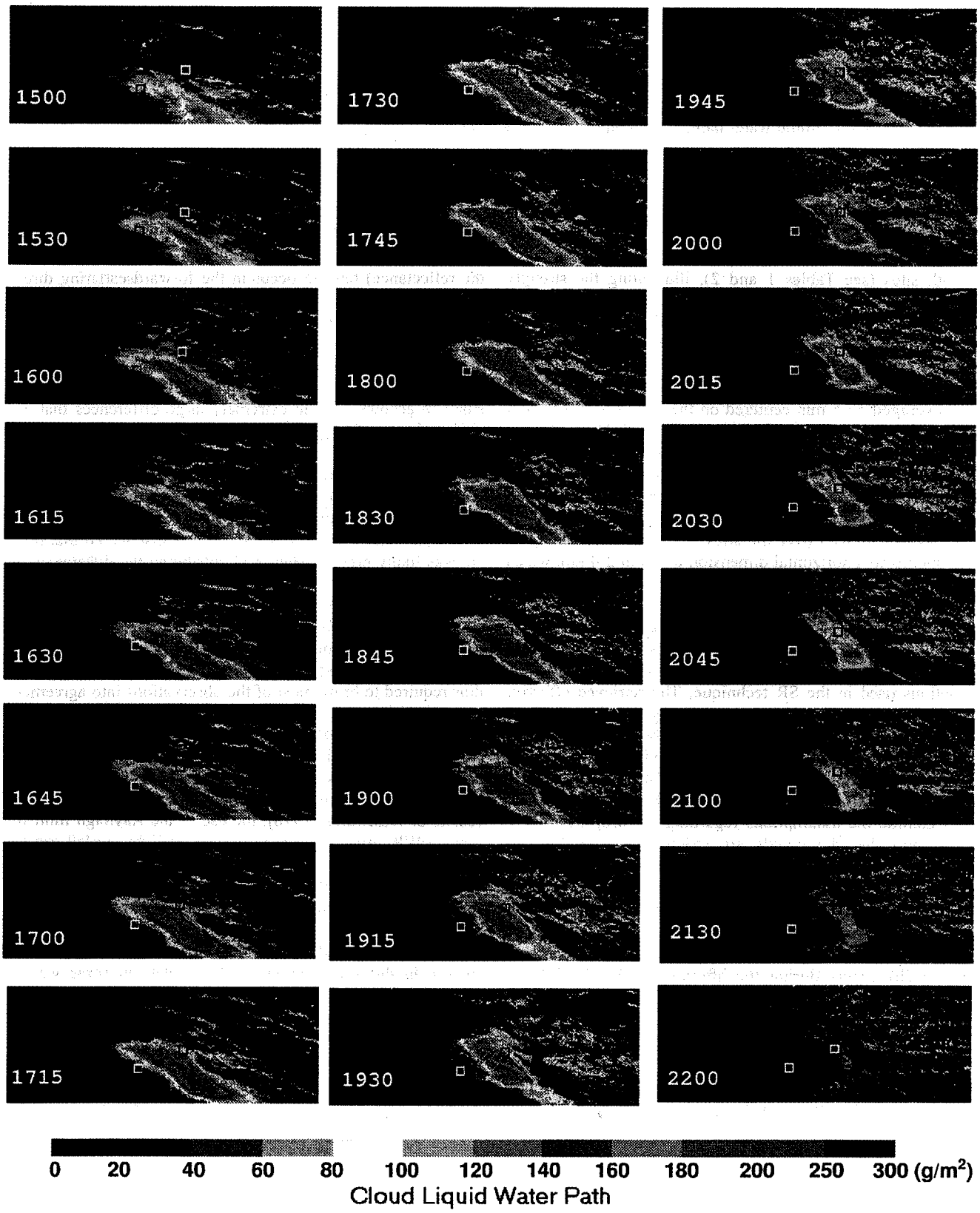

Plate 1. Spatial distribution of cloud LWP over the area of study at various times (UTC) as determined from GOES 9 measurements in the satellite projection. Small squares (white or black) signify locations of Morris and Purcell sites.

Table 1. Summary of Radiosonde Analysis Over Morris, Oklahoma on May 2, 1996

UTC	Cloud Top Height, m	Cloud Base Height, m	Cloud Depth, m	Adiabatic LWP, g m^{-2}	Comments
1430	718	568	150	15	Weak inversion
1730	1271	867	404	110	Very weak inversion
2030	1218	889	329	72	Moderately strong inversion
2330	1053	889	164	18	Moderately strong inversion

LWP, liquid water path; cloud heights above sea level.

early afternoon as observed by the SMWR, even at the Purcell site where the cloud LWP values are often small. In addition, at 1730 UTC, both sets of observations are in very good agreement with the radiosonde-derived adiabatic cloud LWP at both sites (see Tables 1 and 2), illustrating the strongly adiabatic nature of this cloud system in its early stages.

A closer examination of this correspondence at both sites is shown in Figure 4 in the form of a scatter diagram. The comparisons were made for data during 1500-1900 UTC at Morris and 1500-1915 UTC at Purcell. The SMWR observations were averaged ±7.5 min centered on the GOES 9 observation time. Standard deviations were also computed. Naturally, the length of time over which to average these data is somewhat arbitrary. However, a 15-min time average seems reasonable given that the winds in the boundary layer were rather light (about 2.5-4 m s^{-1}), and assuming cloud features remained intact as they moved over the sites, a 15-min period roughly corresponds to a horizontal dimension of about 2-4 km, which is comparable to the spatial scale of the GOES 9 measurements. The linear correlation between these data sets is 0.94 and the root-mean-square difference is 17 g m^{-2}.

The very good agreement between these independent data sets is all that more extraordinary given the simplifying assumptions used in the SR technique. The retrieved effective radius (using 3.7 μm measurements) is generally not representative of the entire depth of the cloud, being within 90% of its cloud top value, though this can depend on the magnitude of r_e at cloud top, the cloud optical depth, and the vertical variation of r_e [*Nakajima and King*, 1990]. Other approximations include the assumptions regarding the drop size distribution and that the clouds are strictly plane-parallel and consist of a single layer. The results of this comparison, however, clearly demonstrate the validity of SR techniques for providing useful quantitative information about cloud LWP, at least for single-layered stratiform clouds.

The most interesting aspect of the comparison at Morris (Figure 2b) occurs during the afternoon (1915-2145 UTC) when there are major disagreements between the observations for three separate events. This is also the time at which the cloud system as a whole appears to have begun its decaying phase. These discrepancies are significant because they may be additional signatures that the cloud system (at least near Morris) is undergoing dramatic microphysical changes. One might propose that these differences might be the result of biases in the GOES 9 optical depth retrievals caused by the application of plane-parallel theory. *Loeb and Coakley* [1998] found that the greatest plane-parallel bias errors (up to 30% in the reflectance) tend to occur in the forwardscattering direction for solar zenith angles greater than 60°. However, during this time period, the solar zenith angles ranged from 20° to 50°, and the measurements were made in the backscattering direction, conditions under which Loeb and Coakley showed the errors to be less than 10%. This effect is therefore too small to account for the extremely large differences that are observed (up to 200 g m^{-2}).

Han et al. [1995] also observed a similar disparity between International Satellite Cloud Climatology Project (ISCCP) derived cloud LWP (using the SR technique) and SMWR for marine stratocumulus on July 9, 1987, during FIRE. Using both ceilometer and SMWR data, it was discovered that drizzle was likely present. Han et al. attributed the differences in retrieved cloud LWP to the underestimation of r_e in the satellite retrievals (hence underestimating cloud LWP).

The differences found by *Han et al.* [1995] for a suspected case of drizzle, although for marine stratocumulus, may have relevance to this study as well. In this study, the effective radius required to bring most of the observations into agreement would be 20 μm or more. However, we believe there is another explanation for these differences that is just as likely. All algorithms used for retrieving cloud LWP from SMWR measurements apply the Rayleigh approximation and thus do not account for extinction by drizzle drops. According to the results of *Westwater* [1978], the use of the Rayleigh limit for cloud LWP retrievals in the presence of light rainfall can result in errors as high as a factor of 2 or 3. However, the degree of overestimation will depend on several factors including the depth of the rain layer and the amount of cloud liquid water [*Sheppard*, 1996].

We suspect the differences that are observed over the Morris site in the afternoon most likely relate in some way to changes in the cloud microphysics and the very different way in which these two types of measurements respond to these changes. Unfortunately, without the benefit of in situ measurements of the drop size spectra within the clouds, it will be very difficult to determine precisely the cause of the observed differences. Nevertheless, we can surmise that there are likely

Table 2. Same as Table 1, Except for Purcell, Oklahoma

UTC	Cloud Top Height, m	Cloud Base Height, m	Cloud Depth, m	Adiabatic LWP, g m^{-2}	Comments
1430	858	598	260	46	Very strong inversion
1730	1215	1070	145	13	Very strong inversion
2030	-	1163	-	-	Very weak inversion
2330	-	-	-	-	Inversion breaks, cloud-free

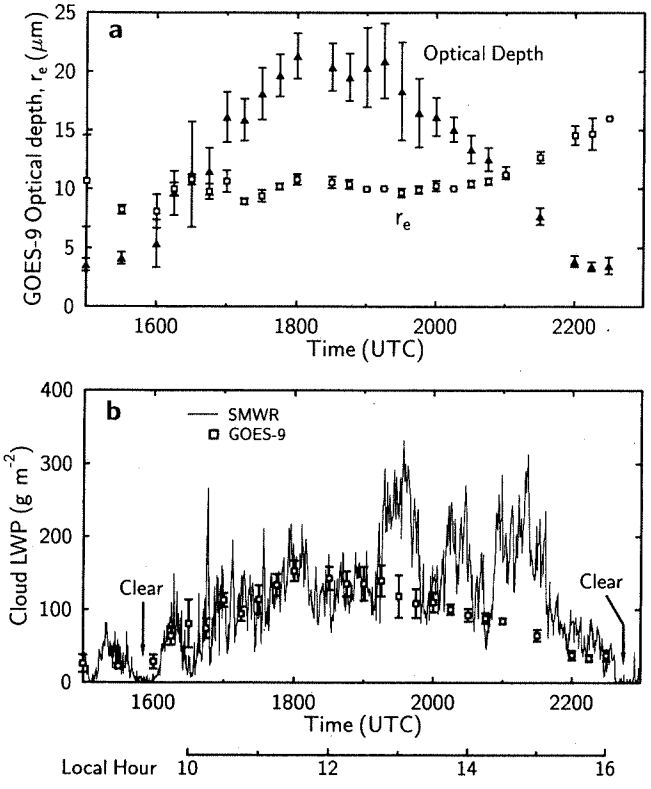

Figure 2. Time series of (a) GOES 9 derived effective radius (r_e) and cloud optical depth retrievals and (b) GOES 9 and surface microwave radiometer (SMWR) cloud liquid water path (LWP) estimates over Morris, Oklahoma.

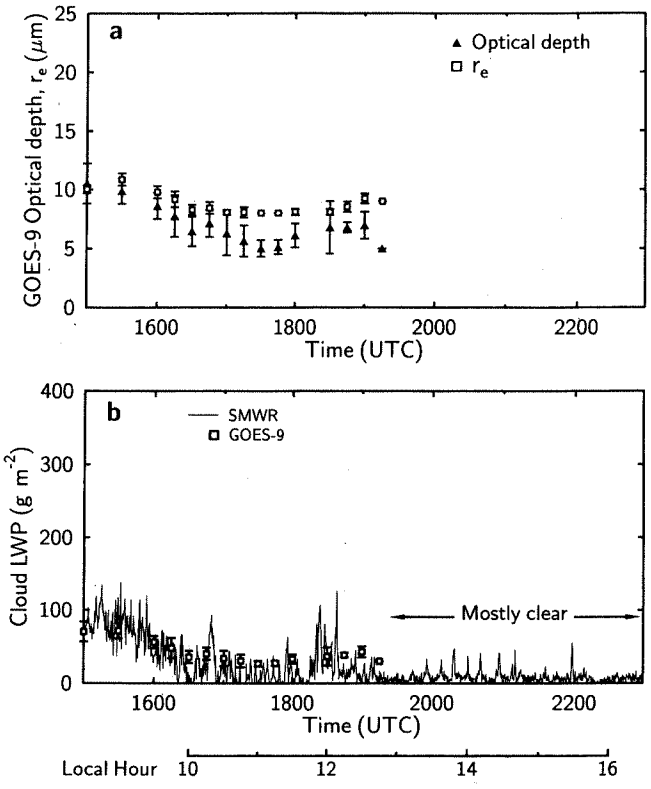

Figure 3. Same as for Figure 2, but Purcell, Oklahoma.

two plausible explanations. Because the effective drop sizes near the cloud top are invariant (as determined from the satellite retrievals) and because the SMWR observations of cloud LWP greatly increase, hence implying the presence of additional liquid water mass, suggests that either drizzle drops or larger cloud droplets have formed in the mid to lower regions of the cloud system.

One experiment to perhaps determine which of these hypotheses is correct is to exploit the small difference in spectral signature between drizzle drops and large cloud droplets at microwave frequencies using simulations and the SMWR brightness temperatures. To simulate the downwelling 23.8 GHz and 31.4 GHz brightness temperatures at the surface, a multistream doubling/adding radiative transfer model was used [*Evans and Stephens*, 1991]. The gaseous and cloud drop attenuation was computed from the millimeter wave propagation model (MPM) of *Liebe* [1981]. For simplicity, the drizzle drops were characterized by a Marshall-Palmer distribution [*Marshall and Palmer*, 1948].

The radiosonde data at 2030 UTC were selected as the test case for the simulations. The cloud was inserted in the model at the heights determined from the radiosonde data (see Table 2). For the purposes of this study, the r_e at cloud top was assigned the value obtained from the GOES 9 retrieval (i.e., 10 μm), though the actual value at cloud top is probably about 10% higher. A value of r_e of 3 μm was assumed at cloud base and r_e varied linearly throughout the cloud depth. A constant total droplet concentration of 270 cm^{-3} was also assumed, a typical value for continental stratocumulus [*Martin et al.*, 1994]. This gave a cloud LWP of 93 g m^{-2} for the simulated cloud that is in excellent agreement with the GOES 9 retrieval at 2030 UTC (93±9 g m^{-2}) but slightly higher than the adiabatic derived LWP (see Table 2). Drizzle drops with the same rainfall rate were inserted at all levels within the model cloud 90 m below cloud top and 630 m below the cloud base (42 m above the surface). A crude calibration of the simulations was achieved using the Morris radiosonde profile at 0830 UTC

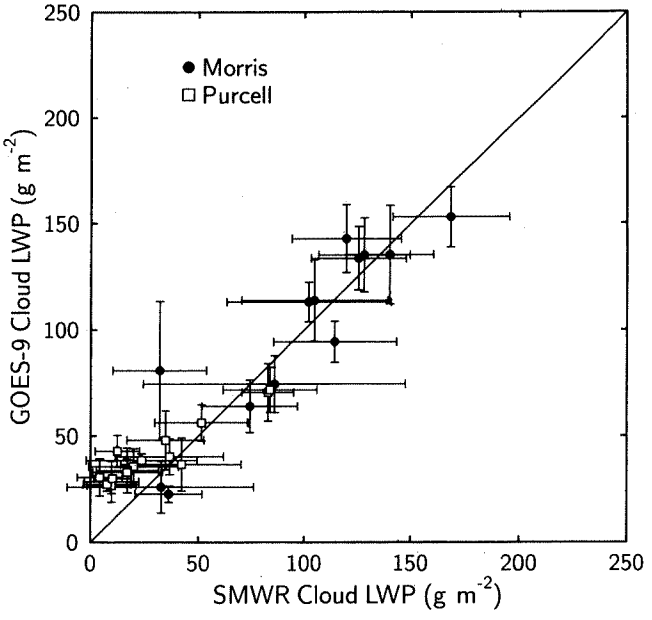

Figure 4. Comparison of GOES 9 and surface microwave radiometer (SMWR) retrievals of cloud LWP over the Morris (1500-1900 UTC) and Purcell sites (1500-1915 UTC). Line of perfect correspondence is also shown.

during a time of known clear-sky conditions. Comparisons of the calculations to the SMWR brightness temperatures showed low biases in the simulations of 1.4 K at 31.4 GHz and 0.4 K at 23.8 GHz. These values were added to the simulation results. Calculations of the 31.4 and 23.8 brightness temperatures were performed separately for rain rates of 0, 0.1, 0.3, 0.5, and 0.7 mm hr^{-1} (typical of drizzle) and r_e values at cloud base ranging from 3 to 10 μm (i.e., liquid water contents of 0.025 to 0.735 g m^{-3}) to represent larger cloud drops.

The results of the simulations and the SMWR observations (1910-2142 UTC) are shown as a bispectral plot (Figure 5). There is an apparent offset of about 2 K between the observed and simulated 23.8 GHz brightness temperatures but this is unimportant in our discussion. Results show that as expected the different responses (i.e., the difference in slopes) between drizzle drops and larger cloud drops is very small (slope of 1.9 versus 1.8, respectively). Although the slope of the measurements (i.e., 1.7) appears to be in closer agreement with the slope for the increase in cloud drop size, the uncertainties in the simulated slopes are rather large because of the lack of knowledge regarding the cloud drop and raindrop size distributions and their vertical variation and the depth of the rain layer. A far larger separation would be needed to differentiate between the simulated slopes for drizzle and cloud drops. The difficulty, of course, is that the difference in extinction between drizzle drops and cloud drops at these frequencies is very small. The use of higher microwave frequencies (such as 90 GHz) along with the lower frequencies would likely be needed to differentiate between these drop sizes.

While the microwave measurements themselves were unable to reveal whether there was drizzle drops or larger cloud droplets, the GOES 9 optical depth retrievals might provide additional clues. If larger cloud liquid water contents were in fact present in the lower portions of the clouds this would greatly increase the extinction at 0.6 μm. Calculations show that an increase in the liquid water content from 0.025 g m^{-3} (r_e=3 um) to 0.735 g m^{-3} (r_e=10 um) at cloud base for a cloud depth of 329 m would nearly double the total extinction coefficient (≈40 to 76 km^{-1}), thus increasing the optical depth from 13 to 38. However, no such increase is observed in Figure 2a; in fact the optical depth steadily decreases. This behavior in the cloud optical depth is quite typical of stratocumulus in which drizzle has formed, owing to a reduction in the cloud droplet number concentration through collision and coalescence, processes that deplete the cloud water content [*Feingold et al.*, 1997]. *Boers et al.* [1996] showed using in situ data for Southern Hemisphere marine stratocumulus that drizzle formation could dramatically reduce the cloud albedo (up to 18%), a result of changes in cloud optical depth. Our results showed a 21% drop in optical depth from the beginning to the end of the first event (1915-1945 UTC). Relative optical depth changes were even larger for the two later events.

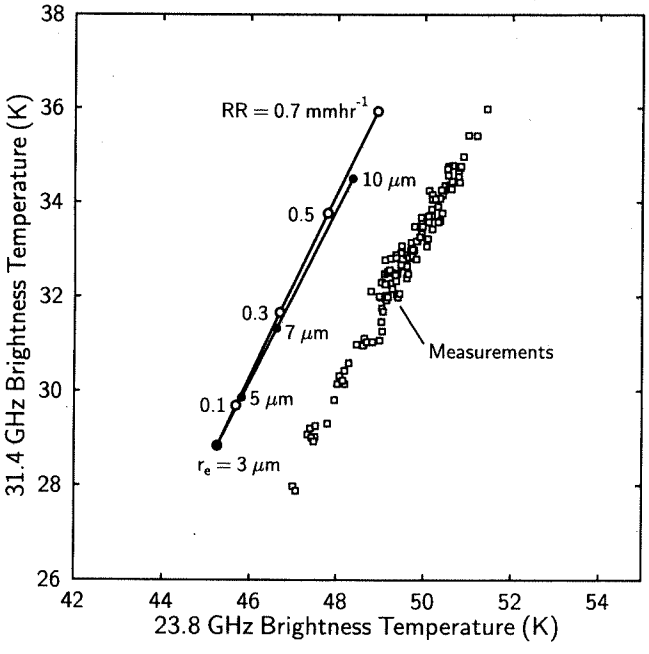

Figure 5. Comparison of 23.8 and 31.4 GHz brightness temperatures simulated for different drizzle rain rates (RR) and cloud drop effective radii (r_e) at cloud base. Also shown are measured data from the surface microwave radiometer at Morris, Oklahoma, during 1910-2142 UTC.

Also consistent with our results is the fact that the direct impact of drizzle on 0.6 μm radiation is anticipated to be unimportant, mainly because of the low total number concentration of drizzle (at least several orders of magnitude less than the total concentration of cloud droplets). For example, *Wiscombe et al.* [1984] examined the difference in absorption from 0.3 to 5 μm between two different realistic drop size distributions derived from a microphysical model; one composed of small droplets only (r_e = 12 μm) and one containing drops as large as raindrops (r_e = 55 μm). The latter distribution was fitted with a Marshall-Palmer distribution for radii beyond 500 μm. Their results showed that the difference in the normalized extinction coefficient at 0.6 μm between these two distributions was about 0.6%, demonstrating the negligible effect of raindrops on radiation at these short wavelengths. At near-infrared wavelengths, in contrast, the effects of larger drops were significant. However, since only minor changes in r_e were observed from GOES 9, the larger drops were probably located in the lower regions of the cloud system where the 3.9 μm radiances are unresponsive.

If drizzle had occurred over Morris in the afternoon, it was most likely light in nature. *Gerber* [1996], using in situ measurements during ASTEX, found that heavy-drizzle marine stratocumulus could be defined by r_e > 16 μm near cloud top and thus proposed it as a means of identifying drizzling clouds from remote sensing. *Han et al.* [1995] applied this idea to marine stratocumulus during FIRE. During the first two episodes of maximum LWP derived from the SMWR (1915-1945 UTC and 2000-2045 UTC), r_e remained essentially constant near 10 μm. It was only during the third episode (2045-2130 UTC) when r_e began to increase. Values of r_e near 16 μm were only reached just before the cloud had nearly completely dissipated. These results are not unexpected because the formation of heavy drizzle in continental stratocumulus is not likely since these clouds generally contain higher droplet number concentrations that classify them in a light drizzle regime [*Gerber*, 1996].

One final attempt was made to determine the existence of drizzle over the Morris site using Next Generation Radar (NEXRAD) Level II data near Tulsa, Oklahoma. Morris is located approximately 70 km SW of the radar location. This new generation of weather radar has doppler capability, a range of 230 km, and is sensitive enough to detect not only

drizzle but also cloud droplets. The base reflectivities (0.5° elevation angle) as measured by NEXRAD in precipitation mode from 1945 to 2218 UTC indicated clouds moving to the east in the NE corner of Oklahoma but quickly disappearing at a range of about 70 km. This occurred because beyond this range the cloud heights were below the altitude of the lowest elevation scan. Therefore the Morris site and the entire cloud system studied in this work were unfortunately just outside the range of detection of the radar.

4. Summary

Study of a continental stratocumulus system using high-temporal resolution surface microwave radiometer and visible/near-infrared satellite measurements and radiosonde data has given a detailed account of the space/time evolution of this cloud system and demonstrated how these different measurement systems can provide unique and complementary information about the cloud system's development and decay. This study differs from previous work in that it is a first attempt to intercompare high-temporal resolution cloud LWP observations over land from independent techniques at geostationary orbit and from surface microwave radiometers. The GOES 9 data were especially valuable in providing a nearly complete history of the cloud system's development, something not possible with data from sun-synchronous satellites.

It was shown that early in the life history of the cloud system both the satellite and SMWR observations of cloud LWP compared very well (root-mean-square difference of 0.17 g m^{-2} and linear correlation of 0.94). This is encouraging given the very different scales of these observations and the simplifying assumptions used in the SR technique. These results are further confirmation of the validity of SR techniques for retrieving cloud LWP for extensive, single-layered stratocumulus. However, large discrepancies between these observations (up to 200 g m^{-2}) occurred at the Morris site immediately following the onset of the cloud system's decaying stage as seen from the satellite imagery. We hypothesized that these differences were most likely due to light drizzle drops that had formed, causing the SMWR cloud LWP retrievals to be overestimated; an idea supported by indirect evidence. Although unavailable at the time of this study, simultaneous millimeter-wave radar measurements, along with aircraft in situ microphysical measurements, would have been extremely useful in identifying drizzle and either confirming or contradicting this hypothesis. Also, using the observations together with boundary layer model simulations containing explicit microphysics might also provide a more complete picture and understanding of the microphysical-radiative interactions and evolution of this cloud system, a task that awaits further study.

It has been suggested that SMWR observations might be useful for validating or testing satellite observations of cloud LWP [e.g., *Greenwald et al.* 1993]. On the basis of this study, however, there are several key issues that need to be addressed before such comparisons can be carried out routinely. First, SMWR observations of cloud LWP sometimes exhibit large systematic errors (up to 50 g m^{-2} as determined from this study). These errors must be accounted for if SMWR observations are to be used as a reliable source of validation. One idea might be to use known clear-sky conditions to adjust the retrievals, as has been done using passive microwave satellite measurements [e.g., *Greenwald et al.*, 1993]. Also, additional work is needed to further understand the effects of drizzle on SMWR measurements, which appear to have a significant impact on the cloud LWP retrievals. While important work has been accomplished on the error analysis of SR retrievals [e.g., *Nakajima and King*, 1990; *Platnick and Valero*, 1995] further work is still needed, such as more aggressively addressing calibration issues (arguably the largest source of systematic error) and fully characterizing the errors for instantaneous retrievals. Moreover, standard procedures should be adopted for dealing with differences in the scale of the various measurement systems (point versus area average) since, depending on the circumstances, large errors can be introduced into the comparisons.

An important outcome of this study is that comparisons of cloud LWP derived from passive microwave systems (whether from ground or satellite) with visible/near-infrared imagers should be performed cautiously. Large differences between these observations might simply indicate that one or the other (or both) measurements are not applicable under certain conditions, and therefore a direct comparison is inappropriate. However, our results also indicate that these differences might be exploited for supplying additional valuable information about microphysical changes in evolving stratocumulus systems. This suggests that such a multisensor, multispectral observing strategy might be feasible for studying marine stratocumulus based solely on satellite measurements, provided there are improvements in the spatial resolution of passive microwave sensors.

Acknowledgments. Financial support for this work was provided by the DoD Center for Geosciences grant DAAL01-98-2-0078 MOD 01. S. Christopher and J. Liljegren were supported by NASA Grant NAGW-5195 and DOE grant CHENG82-1010502-0002884, respectively. The GOES 9 data were acquired through the Cooperative Institute for Research in the Atmosphere at Colorado State University. The ground-based microwave radiometer and radiosonde data were obtained from the Atmospheric Radiation Measurement (ARM) program sponsored by the U.S. Department of Energy, Office of Energy Research, Office of Health and Environmental Research, Environmental Sciences Division. Thanks go to Pete Roohr and Brian Motta for helping us to acquire and display the NEXRAD data. We also acknowledge two anonymous reviewers whose comments helped to improve the manuscript.

References

Albrecht, B. A., C. W. Fairall, D. W. Thompson, A. B. White, J. B. Snider, and W. H. Schubert, Surface-based remote sensing of the observed and the adiabatic liquid water content of stratocumulus clouds, *Geophys. Res. Lett.*, *17*, 89-92, 1990.

Allen, R. C., Jr., P. A. Durkee, and C. H. Wash, Snow/cloud discrimination with multispectral satellite measurements, *J. Appl. Meteorol.*, *29*, 994-1004, 1990.

Basharinov, A. Y., A. S. Gurvich, and S. T. Yegorov, Determination of geophysical parameters from data on thermally-induced radio emission obtained with the Cosmos 243 satellite, *Dokl. Akad. Nauk SSSR*, *188*, 1273-1276, 1969.

Baum, B. A., et al., Imager clear-sky determination and cloud detection, in *Clouds and the Earth's Radiant Energy System (CERES) Algorithm Theoretical Basis Document*, subsyst. 4.1, release 2.1, 44 pp., NASA Langley, Hampton, Va., 1996.

Boers, B., J. B. Jensen, P. B. Krummel, and H. Gerber, Microphyscial and shortwave radiative structure of wintertime stratocumulus clouds over the Southern Ocean, *Q. J. R. Meteorol. Soc.*, *122*, 1307-1339, 1996.

Che, N., and J. C. Price, Survey of radiometric calibration results and methods for visible and near infrared channels of NOAA-7, -9, and -11 AVHRRs, *Remote Sens. Environ.*, *41*, 19-27, 1992.

Evans, K. F., and G. L. Stephens, A new polarized atmospheric radiative transfer model, *J. Quant. Spectrosc. Radiat. Transfer*, *46*, 413-423, 1991.

Feingold, G., R. Boers, B. Stevens, and W. R. Cotton, A modeling study of the effect of drizzle on cloud optical depth and susceptibility, *J. Geophys. Res.*, *102*, 13,527-13,534, 1997.

Fowler, L. D., D. A. Randall, and S. A. Rutledge, Liquid and ice cloud microphysics in the CSU general circulation model, I, Model description and simulated microphysical processes, *J. Clim.*, *9*, 489-529, 1996.

Gerber, H., Microphysics of marine stratocumulus clouds with two drizzle modes, *J. Atmos. Sci.*, *53*, 1649-1662, 1996.

Greenwald, T. J., S. A. Christopher, and J. Chou, Cloud liquid water path comparisons from passive microwave and solar reflectance satellite measurements: Assessment of sub-field-of-view cloud effects in microwave retrievals, *J. Geophys. Res.*, *102*, 19,585-19,596, 1997.

Greenwald, T. J., G. L. Stephens, T. H. Vonder Haar, and D. L. Jackson, A physical retrieval of cloud liquid water over the global oceans using special sensor microwave/imager (SSM/I) observations, *J. Geophys. Res.*, *98*, 18,471-18,488, 1993.

Han, Q., W. B. Rossow, and A. A. Lacis, Near-global survey of effective droplet radii in liquid water clouds using ISCCP data, *J. Clim.*, *7*, 465-497, 1994.

Han, Q., W. B. Rossow, R. M. Welch, A. White, and J. Chou, Validation of satellite retrievals of cloud microphysics and liquid water path using observations from FIRE, *J. Atmos. Sci.*, *52*, 4183-4195, 1995.

Hill, G., Analysis of supercooled liquid water measurements using microwave radiometer and vibrating wire devices, *J. Atmos. Oceanic Technol.*, *11*, 1242-1252, 1994.

Kaufman, Y. J., and B. N. Holben, Calibration of the AVHRR visible and near-IR bands of atmospheric scattering, ocean glint and desert reflection, *Int. J. Remote Sens.*, *14*, 21-52, 1993.

Kneizys, F. X., *Users guide to LOWTRAN-7*, *Environ. Res. Pap., No. 1010*, 137 pp., Air Force Geophys. Lab., Hanscom AFB, Mass., 1988.

Lemus, L., L. Rikus, C. Martin, and R. Platt, Global cloud liquid water path simulations, *J. Clim.*, *10*, 52-64, 1997.

Liebe, H. J., Modeling attenuation and phase of radio waves in air at frequencies below 1000 GHz, *Radio Sci.*, *16*, 1183-1199, 1981.

Liljegren, J. C., Improved retrieval of cloud liquid water path, paper presented at proceedings of 10th Symposium on Meteorological Observations and Instrumentation, Phoenix, Arizona, Am. Meteorol. Soc., 1998.

Loeb, N. G., and J. A. Coakley Jr., Inference of marine stratus cloud optical depths from satellite measurements: Does 1D theory apply?, *J. Clim.*, *11*, 215-233, 1998.

Marshall, J. S., and W. M. Palmer, The distribution of raindrops with size, *J. Meteorol.*, *5*, 165-166, 1948.

Martin, G. M., D. W. Johnson, and A. Spice, The measurement and parameterization of effective radius of droplets in warm stratocumulus clouds. *J. Atmos. Sci.*, *51*, 1823-1842, 1994.

Menzel, P. W., and J. F. W. Purdom, Introducing GOES I: The first of a new generation of geostationary operational environmental satellites, *Bull. Am. Meteorol. Soc.*, *75*, 757-781, 1994.

Minnis P., P. W. Heck, D. F. Young, C. W. Fairall, and J. B. Snider, Stratocumulus cloud properties derived from simultaneous satellite and island-based instrumentation during FIRE, *J. Appl. Meteorol.*, *31*, 317-339, 1992.

Nakajima, T., and M. D. King, Determination of the optical thickness and effective particle radius of clouds from reflected solar radiation measurements, I, Theory, *J. Atmos. Sci.*, *47*, 1878-1893, 1990.

Nakajima, T. Y., and T. Nakajima, Wide-area determination of cloud microphysical properties from NOAA AVHRR measurements for FIRE and ASTEX regions, *J. Atmos. Sci.*, *52*, 4043-4059, 1995.

Nakajima, T., M. D. King, J. D. Spinhirne, and L. F. Radke, Determination of the optical thickness and effective particle radius of clouds from reflected solar radiation measurements, II, Marine stratocumulus observations, *J. Atmos. Sci.*, *48*, 728-750, 1991.

Paltridge, G. W., Cloud-radiation feedback to climate, *Q. J. R. Meteorol. Soc.*, *106*, 895-899, 1980.

Platnick, S., and F. P. J. Valero, A validation of a satellite cloud retrieval during ASTEX, *J. Atmos. Sci.*, *52*, 2985-3001, 1995.

Prabhakara, C., I. Wang, A.T.C. Chang, and P. Gloerson, A statistical examination of Nimbus-7 SMMR data and remote sensing of sea surface temperature, liquid water content in the atmosphere and surface wind speed, *J. Clim. Appl. Meteorol.*, *22*, 2023-2037, 1983.

Ramaswamy, V., and C.-T. Chen, An investigation of the global solar radiative forcing due to changes in cloud liquid water path, *J. Geophys. Res.*, *98*, 16,703-16,712, 1993.

Roeckner, E., U. Schlese, J. Biercamp, and P. Loewe, Cloud optical depth feedbacks and climate modeling, *Nature*, *329*, 138-140, 1987.

Sheppard, B. E., Effect of rain on ground-based microwave radiometric measurements in the 20-90-GHz range, *J. Atmos. Oceanic Technol.*, *13*, 1139-1151, 1996.

Somerville, R. C. J., and L. A. Remer, Cloud optical thickness feedbacks in the CO_2 climate problem, *J. Geophys. Res.*, *89*, 9668-9672, 1984.

Stokes, G. M., and S. E. Schwartz, The Atmospheric Radiation Measurement (ARM) program: Programmatic background and design of the cloud and radiation test bed, *Bull. Am. Meteorol. Soc.*, *75*, 1201-1221, 1994.

Taylor, V. R., and S. J. Ghan, An analysis of cloud liquid water feedback and global climate sensitivity in a general circulation model, *J. Clim.*, *5*, 907-919, 1992.

Westwater, E. R., The accuracy of water vapor and cloud liquid water determination of dual-frequency ground-based microwave radiometery, *Radio Sci.*, *13*, 677-685, 1978.

Wiscombe, W. J., R. M. Welch, and W. D. Hall, The effects of very large drops on cloud absorption. Part I: Parcel models, *J. Atmos. Sci.*, *41*, 1336-1355, 1984.

S. A. Christopher and J. Chou, Department of Atmospheric Sciences, University of Alabama in Huntsville, 977 Explorer Boulevard, Huntsville, AL 35807.

T. J. Greenwald, Cooperative Institute for Research in the Atmosphere (CIRA), Colorado State University, Fort Collins, CO 80523. (greenwald@cira.colostate.edu)

J. C. Liljegren, DOE Ames Laboratory, Center for NDE, 1915 Scholl Road, Ames, IA 50011.

(Received August 17, 1998; revised December 11, 1998; accepted January 15, 1999.)